

Self-supervised and Weakly Supervised Contrastive Learning for Frame-wise Action Representations

Minghao Chen^{*†}, Renbo Tu^{*}, Chenxi Huang, Yuqi Lin, Boxi Wu, and Deng Cai

Abstract—Previous work on action representation learning focused on global representations for short video clips. In contrast, many practical applications, such as video alignment, strongly demand learning the intensive representation of long videos. In this paper, we introduce a new framework of contrastive action representation learning (CARL) to learn frame-wise action representation in a self-supervised or weakly-supervised manner, especially for long videos. Specifically, we introduce a simple but effective video encoder that considers both spatial and temporal context by combining convolution and transformer. Inspired by the recent massive progress in self-supervised learning, we propose a new sequence contrastive loss (SCL). It optimizes embedding space by minimizing cross-entropy between sequence similarity of two augmented views and prior Gaussian distribution of timestamp distance. In weakly-supervised learning, we design paired contrastive loss (PCL) using dynamic time warping (DTW) in ensemble views with video-level labels. Experiments on PennAction, FineGym, and Pouring datasets show that our method outperforms previous state-of-the-art by a large margin for downstream fine-grained action classification and has better speed and memory cost. Surprisingly, although without training on paired videos like in previous works, our self-supervised version also shows outstanding performance in video alignment and fine-grained frame retrieval tasks. Our weakly-supervised version further improves the performance.

Index Terms—Representation Learning, Video Analysis, Long Video, Transformer, Contrastive Learning, Self-supervised Learning, and Weakly supervised Learning.

1 INTRODUCTION

RECENTLY, deep learning of video understanding has received extensive attention [1], [2], [3], [4], [5], [6], [7], [8] and has achieved great success in video classification tasks [2], [9], [10]. Networks such as I3D [2] and SlowFast [3] take short video clips (e.g., 32 or 64 frames) as input and extract global representations to predict the action category. In contrast, many practical applications, e.g., sign language translation [11], [12], [13], robotic imitation learning [14], [15], action alignment [16], [17], [18], and phase classification [19], [20], [21], [22], require algorithms to have the ability to model fine-level representation in long videos with hundreds of frames. Therefore, we designed a new framework to extract frame-wise representation rather than global features.

Previous methods [20], [21], [23] have made an effort to learn frame-wise representations via supervised learning, where sub-actions or phase boundaries are annotated. However, it is time-consuming and impractical to manually label each frame and exact action boundaries, especially on large-scale datasets. It hinders the generalization of models trained with fully supervised learning in realistic scenarios. To reduce the dependency on labeled data, some methods, such as TCC [19], LAV [18] and GTA [17], explored weakly-

supervised learning using either cycle-consistency loss [17], [19] or soft dynamic time warping [17], [18], [24]. All these methods rely on video-level annotations, and the training is conducted on the paired videos describing the same action. Motivated by contrastive learning, our framework can learn the frame-wise representation and perform better without video pairs and supervision.

In this work, we aim to learn frame-wise representations with spatio-temporal context for long videos in a self-supervised or weakly-supervised manner. Inspired by contrastive representation learning [25], [26], [27], [28], we present a novel framework named contrastive action representation learning (CARL). Our work can be done without supervision and video pairs, which are time-consuming and hard to get. Surprisingly, the performance of our work is much better than previous work. The performance can be even better if we take weak supervision, which only uses video-level labels that can be easily obtained. Thus it is practical to scale up our training set with less cost.

Modeling long videos with hundreds of frames is challenging as the memory is limited. It is non-trivial to use off-the-shelf backbones designed for short video clips directly. In our work, we mainly utilize the global relationship modeling and long-distance modeling capabilities of the Transformer [29] to obtain the temporal features of long videos. So, we design a simple yet efficient video encoder that consists of a 2D network to encode spatial information per frame and a Transformer encoder to model temporal interaction. The frame-wise features are then used for representation learning.

Recently, contrastive learning in self-supervised learn-

- Renbo Tu is with the Computer Science department of University of Toronto. E-mails: rtu0715@gmail.com
- Minghao Chen, Chenxi Huang, Yuqi Lin, Boxi Wu, and Deng Cai are with the State Key Laboratory of CAD&CG, College of Computer Science, Zhejiang University, Hangzhou, Zhejiang 310058, China. E-mails: minghaochen01@gmail.com, hcx_98@zju.edu.cn, linyq5566@gmail.com, wuboxi@zju.edu.cn, caideng@cad.zju.edu.cn.
- ^{*} Equal contribution. [†] Corresponding author.

ing has gotten much attention. A typical example is SimCLR [26], which has used instance discrimination [30] as the pretext task and introduced a contrastive loss named NT-Xent. It regards two augmented views of the same video sequence as a positive pair and maximizes their agreement. In their implementation, all instances other than the positive reference are considered negatives. Unlike image data (each image is regarded as an instance), videos provide more abundant instances (each frame is regarded as an instance), and the neighboring frames have high semantic similarities. Directly regarding these frames as negatives may hurt learning. To avoid this issue, we present a novel sequence contrastive loss (SCL), which optimizes the embedding space by minimizing the cross-entropy between the sequence similarity of two augmented video views and a prior Gaussian distribution.

Meanwhile, we design a weak supervision version of SCL by adding video-level labels. Therefore, we can establish more positive and negative pairs among videos for sufficient learning. At the same time, we add a CLS token and a video-level classifier, using weak labels in supervised learning. In this way, the performance improves by a big step, exceeding our self-supervised version by 3% in fine-grained action classification. Compared with previous weakly-supervised methods [17], [18], our performance is faster and higher. We drop out soften DTW, which is designed for back-propagation of DTW. It is because the gradient cost of soft DTW is at least $\min(|V1|, |V2|)$, and at most $|V1| + |V2|$ iteration, which is even worse for long videos. Moreover, we add a class token in our designed video encoder for video-level label supervised learning.

The main contributions of this paper are summarized as follows:

- We propose a novel framework named contrastive action representation learning (CARL) to learn frame-wise action representations with spatio-temporal context information for long videos in a self-supervised manner. We design three modules for learning more general representations: a series of spatio-temporal data augmentations, a Transformer-based network to efficiently encode long videos, and a novel sequence contrastive loss (SCL) for representation learning.
- Using video-level labels, we re-design the Sequence Contrastive Learning module and propose paired contrastive loss (PCL). We not only care about the relationship in the same video but also learn about the relationship between videos. Compared to the previous works that utilize soft DTW, our method is much more training efficient.
- Our framework outperforms the state-of-the-art methods by a large margin on multiple tasks across different datasets. For example, under the linear evaluation protocol on FineGym [21] dataset, our framework achieves 41.75% accuracy, which is +13.94% higher than the existing best method GTA [17]. On Penn-Action [31] dataset, our method achieves 91.67% for fine-grained classification, 99.1% for Kendall's Tau, and 90.58% top-5 accuracy for fine-grained frame retrieval, which all surpass the ex-

isting best methods. With video-level labels, our weakly-supervised manner can get further improved.

An earlier version [32] of this paper was presented at the Conference on Computer Vision and Pattern Recognition (CVPR) 2022. This paper presents a substantial improvement with the following improvements: 1) We consider the weakly supervised learning setting, where the video-level action label of each video is given, and frame-level labels are absent. We propose an improved sequential contrastive loss that views frames from other videos with different action labels as points at infinity. For the videos with the same action labels, we propose a new paired contrastive loss that uses view ensemble and dynamic time warping to find the corresponding frames. 2) We propose more analysis and evaluation metrics of our methods, including the training speed and memory cost of our methods, one-shot phase classification results, and clustering performance. Compared to previous methods, we find our methods are training efficient and achieve new SOTAs under all metrics. 3) We show that we can perform self-supervised pretraining on large-scale datasets, e.g. Kinetics-400, to pretrain the frame-wise action representation. The weight initial from this large-scale pretraining can achieve better performance and generability to downstream tasks.

2 RELATED WORKS

2.1 Conventional Action Recognition

[2], [10], [33], [34], [35] build several challenging video datasets to analyze various scenes and situations. These datasets provide labels of high-level concepts or detailed physical aspects for short videos or clips. Action recognition is a visual task, which requires accurately distinguishing the motion of objects. To solve video recognition, a large number of architectures have been proposed [1], [2], [3], [4], [5], [6], [7], [36], [37]. Most networks are based on 3D Convolution layers and combine with the techniques in image recognition [2], [3], [6], such as residual connection [38] and ImageNet pre-training [39]. However, with the deepening of research, some works [4], [7] find that the insufficient receptive field of 3D ConvNets would limit the understanding of videos and increase the computational budget.

Recently, Transformers [29] has achieved great success in the field of computer vision, such as ViT [40] and DETR [41]. Some works extend Transformers to video recognition, such as TimeSformer [36] and ViViT [1]. Due to the powerful ability and global receptive field of the Transformers, these methods have become new state-of-the-art. For example, combined with a 2D backbone and a Transformer, VTN [4] can effectively process long video sequences. However, these architectures are all designed for video classification and predict one global class for a video.

In this work, combined with transformers, we design a new frame-level video encoder network for fine-level action representations.

2.2 Representation learning in videos

Previous methods of self-supervised learning in videos construct pretext tasks, including predicting temporal transfor-

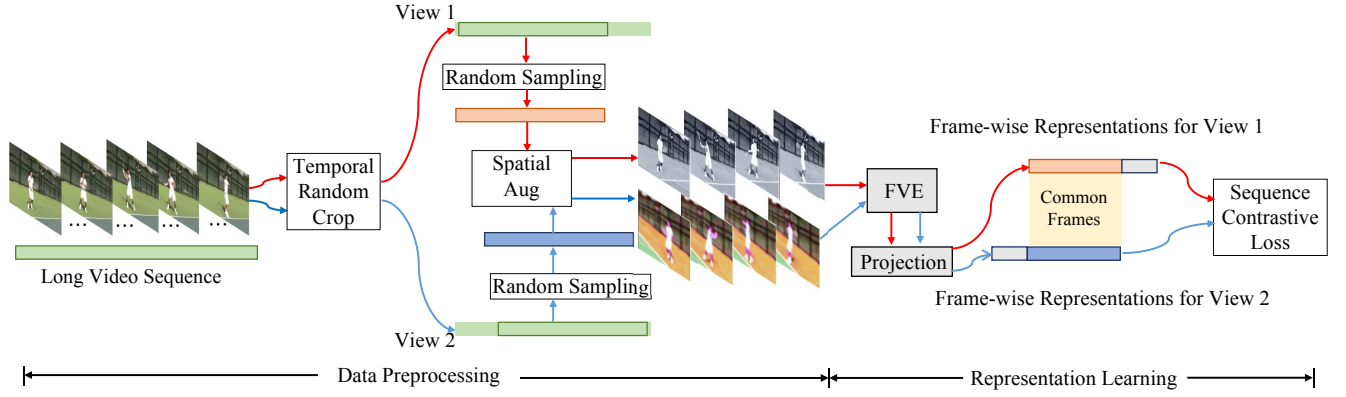


Fig. 1. Overview of our framework (CARL) in self-supervised learning. Two augmented views are constructed from a training video through a series of spatio-temporal data augmentations. The frame-level video encoder (FVE) and the projection head are optimized by minimizing the proposed sequence contrastive loss (SCL) between two views.

mations [42], [43], [44], [45], inferring the future [46], constructing different views [15], [47], [48], and discriminating shuffled frames [49]. [42] investigates 4 different temporal transformations of a video: speed variation, random permutation, Periodic, and Warp. [43], [44] randomly sample training clips at different paces and ask a neural network to identify the pace for each video clip. [45] roots in a dilated sampling strategy, which produces self-supervision signals about video playback rates for representation model learning. There are also some alignment-based methods, where a pair of videos are trained with cycle-consistent loss [19], [50]. [19] design a differentiable cycle-consistency loss that can be used to find correspondences across time in multiple videos. The resulting per-frame embeddings can be used to align videos by simply matching frames using nearest neighbors in the learned embedding space. [17] uses the global temporal ordering of latent correspondences across sequence pairs as a supervisory signal and designs smooth DTW. [50] points out that a good video representation is supposed to be closed across both domains yet distant from all the other videos and frames in the corresponding domain, respectively. And it designs cycle-contrastive loss to learn video representation with the above desired properties.

2.3 Contrastive learning in videos

The contrastive loss, which was first proposed in [51] and later popularized as InfoNCE loss by [52], involves positive and negative pairs of features. It aims to maximize the similarity of positive pairs, which are obtained by generating different views of the same data, and minimize the similarity of negative pairs. For example, [46] and the follow-up work [53] obtain hard negatives from different spatio-temporal locations in the feature map, while [54] constructs negatives based on past and future clips.

Recently, the contrastive learning methods [26], [27], [28], [55] based on instance discrimination have shown superior performance on 2D image tasks. Some works [15], [22], [56], [57], [58] also use this contrastive loss for video representation learning. They treat different frames in a video [15], [22],

[57] or different clips [56], [58] in other videos as negative samples. Different from these methods, our goal is the fine-grained temporal understanding of videos, and we treat a long sequence of frames as input data. The most relevant work to ours is [59], which utilizes 3D human keypoints for self-supervised action discovery in long kinematic videos.

3 METHOD

In this section, we introduce a novel framework named contrastive action representation learning (CARL) to learn frame-wise action representations in self-supervised and weakly-supervised manners. In particular, our framework is designed to model long video sequences by considering the spatio-temporal context. We first present an overview of the proposed framework in Section 3.1. Then we introduce the details of view construction and spatio-temporal data augmentation in Section 3.2. Next, we describe our frame-level video encoder in Section 3.3. Afterward, the proposed sequence contrastive loss (SCL) without any supervision and its design principles are introduced in Section 3.4. Finally, we specially modify the SCL method for weak supervision in Section 3.5.

3.1 Overview

Our method is based on contrastive learning. The definition of positive and negative pairs is most important. The primary process can be concluded as Data Preprocessing and Representation Learning. We first construct two augmented views for each video through a series of spatio-temporal data augmentations. Then, we feed these two augmented views into our frame-level video encoder (FVE) to extract dense representations as Figure 2 shows. Following SimCLR [26], we attach a lightweight projection network after FVE, a two-layer MLP, for obtaining latent embeddings.

In self-supervised learning, we only conduct contrastive learning within a video sequence to obtain a good representation of the video. We adopt the fact that adjacent temporal frames are highly correlated and assume that the similarity distribution between two augmented views from the same video should follow a prior Gaussian distribution.

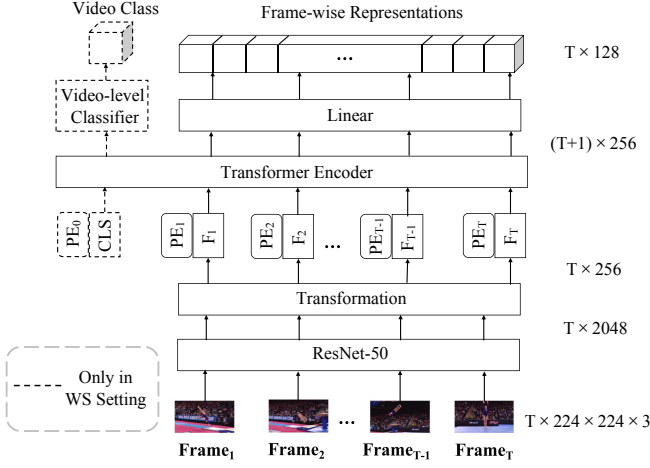


Fig. 2. Architecture of the proposed frame-level video encoder (FVE). The input is a long video with T frames and the outputs are frame-wise representations. ResNet-50 is pre-trained on ImageNet. We freeze the first four residual blocks of ResNet-50 and only finetune the last block. For the weakly-supervised version, we add a class token and a video-level classifier to predict the category of the video.

Based on this assumption, we propose a novel sequence contrast loss (SCL) to optimize frame-wise representation in the embedding space. Figure 1 displays an overview of our framework in unsupervised learning.

However, the above framework only conducts contrastive learning between the two views of the same video sequence and ignores the relationship among videos. More positive and negative samples can be formed by frames from the same batch of videos. It is equivalent to enlarging the batch size and increasing both the number of positive and negative pairs for contrastive learning. The main challenge is that the frames in other videos may have the same action as the current frame, and there is no frame-level label in most datasets.

We solve this problem by using weak labels, that is, video-level labels. Video-level labels are used to describe the semantic information of a video in one sentence. Compared with frame-level labels, they do not focus on specific details and processes. In addition to the positive samples defined in the self-supervised manner, they should also include frames with the same frame-level label in other videos. Concretely, we can select videos with the same video-level label first and then find their corresponding frames. Figure 4 shows an overview of our framework in weakly supervised learning.

3.2 View Construction

We first introduce the view Construction step of our method, as shown in the “Data preprocessing” section in Figures 1 and 4. Data augmentation is essential to avoid trivial solutions both in self-supervised learning and weakly-supervised learning. It can reduce the influence of noise and background on learning essential characteristics. Unlike previous methods [26], [27] designed for image data that only care about spatial augmentations, we introduce a series of spatio-temporal data augmentations for video data to increase the diversity of videos further.

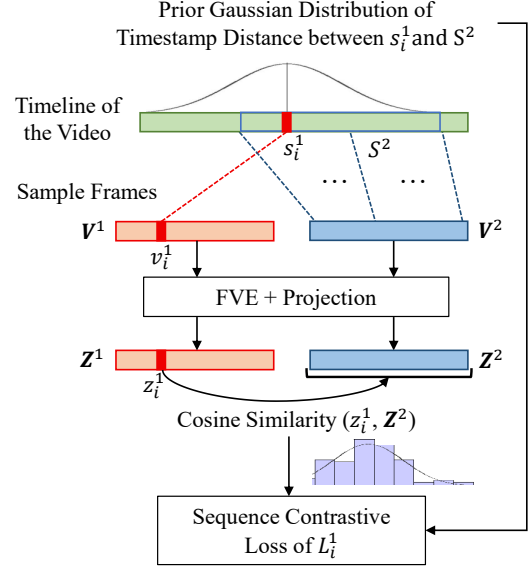


Fig. 3. Illustration of the proposed sequence contrastive loss (SCL). We use the loss computation of $\mathbf{v}_i^1 \in \mathbf{V}^1$ as the example. We first compute a prior Gaussian distribution of timestamp distance ($s_i^1 - s_1^2, \dots, s_i^1 - s_T^2$). Then the embedding similarity distribution between \mathbf{z}_i^1 and \mathbf{Z}^2 is calculated. We minimize the cross-entropy between the embedding similarity of two augmented views.

Specifically, for a training Video \mathbf{V} with S frames, we aim to construct two augmented videos with T frames independently, through a series of spatio-temporal data augmentations. For temporal data augmentation, we first perform temporal random clipping on Video \mathbf{V} to generate two video clips with a length of $[T, \alpha T]$, where α is a hyper-parameter that controls maximum crop size. In this process, we guarantee at least β percent of overlapped frames existing between two clips to form positive pairs subsequently. Then, we randomly sample T frames for each video clip and then obtain two augmented views: $\mathbf{V}^1 = \{\mathbf{v}_i^1 | 1 \leq i \leq T\}$, and $\mathbf{V}^2 = \{\mathbf{v}_i^2 | 1 \leq i \leq T\}$, where \mathbf{v}_i^1 and \mathbf{v}_i^2 represent the i -th frames of \mathbf{V}^1 and \mathbf{V}^2 , respectively. By default, we set $T = 240$ according to the original length of most videos in our used three datasets. Finally, we apply several temporal-consistent spatial data enhancements to \mathbf{V}^1 and \mathbf{V}^2 , independently, including random resize and crop, horizontal flip, random color distortions and random Gaussian blur.

3.3 Frame-level Video Encoder Network

Due to the substantial computational cost, it is non-trivial to directly apply video classification backbones to model long video sequences with hundreds of frames. Previous works [17], [18], [19] primarily used the same video encoder that combines a 2D backbone and several 3D Convolutional layers to generate frame-wise features. However, stacking too many 3D Convolutional layers leads to unaffordable computational costs. Moreover, receptive fields of convolution are local, which is limited to capturing temporal context. Recently, Transformers [29] achieved significant progress in computer vision [40], [41]. Transformers utilize the attention mechanism to solve sequence-to-sequence tasks. The long-range dependencies of the Transformer can

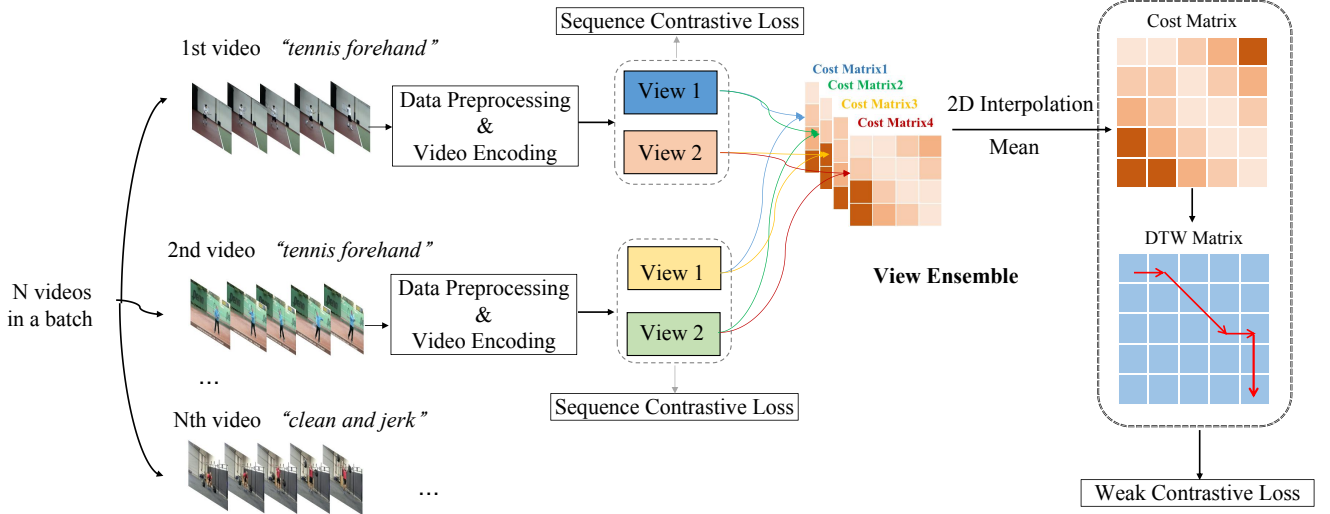


Fig. 4. Overview of our framework (CARL) in weakly-supervised learning. Compared with the self-supervised version, we computed the weak contrastive loss between videos by ensembling views and dynamic time warping (DTW).

benefit sequence data like language, videos, etc. In our network implementation, we adopt the Transformer encoder as an alternative to model temporal context.

In Figure 2, we show our frame-level video encoder (FVE). After seeking the trade-off between representation performance and inference speed, we first use a 2D network, e.g., ResNet-50 [38], to extract spatial features for the RGB video sequence of size $T \times 224 \times 224 \times 3$. Then a transformation block that consists of two fully connected layers with batch normalization and ReLU is applied to project the spatial features to the intermediate embeddings of size $T \times 256$. Following standard practice, we add the sine-cosine positional encoding [29] on top of the intermediate embeddings to encode the temporal order information. Next, the encoded embeddings are fed into the 3-layer Transformer encoder to model temporal context. At last, a linear layer is adopted to obtain the final frame-wise representations $\mathbf{H} \in \mathbb{R}^{T \times 128}$. We use \mathbf{h}_i ($1 \leq i \leq T$) to denote the representation of the i -th frame. For the weakly-supervised version, we add an extra class token. The feature vectors after the transformer encoder are sent to the video-level classifier to predict the category of the video in supervised learning.

The 2D ResNet-50 network is pre-trained on ImageNet [39]. Considering the limited computational budget, we freeze the first four residual blocks since they already learned favorable low-level visual representations by pre-training. This simple design ensures that our network can be trained and tested on videos with more than 500 frames. VTN [4] uses a similar hybrid Transformer-based network to perform video classification. They use the [CLS] token to generate a global feature, while our network is designed to extract frame-wise representations by considering the spatio-temporal context. In addition, our network explores modeling much more prolonged video sequences.

3.4 Sequence Contrastive Learning

SimCLR [26] introduces a contrastive loss named NTXent by maximizing agreement between augmented views of

the same instance. However, unlike images, videos contain much sequential information, which is a vital supervisory signal. For typical instance discrimination, all instances other than the positive reference are considered negatives. Moreover, the neighboring frames around the reference frame are highly correlated. Directly regarding other frames as negatives may hurt learning. Therefore, we should be carefully designed learning principles to avoid this issue. To optimize frame-wise representations, we propose a novel sequence contrastive loss (SCL), as shown in Figure 3. It assumes that the similarity between frames is based on the prior Gaussian distribution in distances. The objective goal is to minimize the cross-entropy between the embedding similarity of augmented views and the prior Gaussian distribution.

Specifically, following SimCLR, we add a small projection network $g(\cdot)$ composed of two-layer MLP after our FVE. The frame-wise representations \mathbf{H} are projected into latent embeddings $\mathbf{Z} = g(\mathbf{H})$. Let $\mathbf{Z}^1 = \{\mathbf{z}_i^1 | 1 \leq i \leq T\}$ and $\mathbf{Z}^2 = \{\mathbf{z}_i^2 | 1 \leq i \leq T\}$, where \mathbf{z}_i^1 and \mathbf{z}_i^2 represent the latent embedding of the i -th frame in Video \mathbf{V}^1 and \mathbf{V}^2 , respectively. Let $\mathbf{S}^1 = \{s_i^1 | 1 \leq i \leq T\}$, which represents the timestamp vector of \mathbf{V}^1 , where s^1 is the corresponding original video timestamp of the i -th frame in \mathbf{V}^1 (see Figure 3). Similarly, we can define $\mathbf{S}^2 = \{s_i^2 | 1 \leq i \leq T\}$.

Given the i -th reference frame in \mathbf{V}^1 and its corresponding latent embedding \mathbf{z}_i^1 , since temporally adjacent frames are more highly correlated than those far-away ones, we assume the embedding similarity between \mathbf{z}_i^1 and $\mathbf{Z}^2 = \{\mathbf{z}_i^2 | 1 \leq i \leq T\}$ should follow a prior Gaussian distribution of timestamp distance between s_i^1 and $\mathbf{S}^2 = \{s_i^2 | 1 \leq i \leq T\}$. This assumption motivates us to use cross-entropy to optimize the embedding space. Specifically, let $\text{sim}(\mathbf{u}, \mathbf{v}) = \frac{\mathbf{u}^T \mathbf{v}}{(\|\mathbf{u}\| \|\mathbf{v}\|)}$ denote cosine similarity, and $\mathbf{G}(x) = \frac{1}{\sigma\sqrt{2\pi}} \exp(-\frac{x^2}{2\sigma^2})$ denotes the Gaussian function, where σ^2 is the variance. We formulate the loss of i -th

reference frame in \mathbf{V}^1 as follows:

$$L_{SCL,i}^1(V) = - \sum_{j=1}^T w_{i,j} \log \frac{\exp(\text{sim}(\mathbf{z}_i^1, \mathbf{z}_j^2)/\tau)}{\sum_{k=1}^T \exp(\text{sim}(\mathbf{z}_i^1, \mathbf{z}_k^2)/\tau)} \quad (1)$$

$$w_{i,j} = \frac{\mathbf{G}(s_i^1 - s_j^2)}{\sum_{k=1}^T \mathbf{G}(s_i^1 - s_k^2)}$$

where $w_{i,j}$ is the normalized Gaussian weight and τ is the temperature parameter. Then the overall loss for \mathbf{V}^1 can be computed across all frames:

$$L_{SCL}^1(V) = \frac{1}{T} \sum_{i=1}^T L_{SCL,i}^1 \quad (2)$$

Similarly, we can calculate the loss L_{SCL}^2 for \mathbf{V}^2 . Our sequence contrastive loss is defined as $L_{SCL}(V) = L_{SCL}^1 + L_{SCL}^2$. Noticeably, our loss does not rely on frame-to-frame correspondence between \mathbf{V}^1 and \mathbf{V}^2 , which supports the diversity of spatial-temporal data augmentation.

3.5 Contrastive Learning with Weak Supervision

In Section 3.4, we only compared and learned frames in the same video \mathbf{V} with different views (compared \mathbf{V}^1 with \mathbf{V}^2) but ignored other videos' information. If we can access video-level labels (y) of training videos, then we can utilize this weak supervision to prompt the frame representation. In this section, we will expand the scope of contrastive learning from self-supervised learning to weakly-supervised learning.

For two videos in a training batch, we separately design loss functions based on whether they belong to the same video-level class. If Video \mathbf{V}_b has different video-level class labels compared with Video \mathbf{V}_a ($y_a \neq y_b$)¹, we can regard that the frames in Video \mathbf{V}_b are infinitely away from the current video frame $\mathbf{V}_{a,i}$. Specifically, SCL for the frames having different video-level classes is defined as follows:

$$L_{SCL,i}^1(V_a) = - \sum_{j=1}^T w_{i,j} \log \frac{\exp(\text{sim}(\mathbf{z}_{a,i}^1, \mathbf{z}_{a,j}^2)/\tau)}{\sum_{\hat{\mathbf{z}} \in \Omega_a} \exp(\text{sim}(\mathbf{z}_{a,i}^1, \hat{\mathbf{z}})/\tau)} \quad (3)$$

$$w_{i,j} = \frac{\mathbf{G}(s_i^1 - s_j^2)}{\sum_{k=1}^T \mathbf{G}(s_i^1 - s_k^2)}$$

$$\Omega_a = \{\mathbf{z} | \mathbf{z} \in Z_a^2 \text{ or } \mathbf{z} \in Z_b^2, y_a \neq y_b\}$$

Comparing Eq 3 with Eq 1, we can find that the main difference is the denominator. In this way, we add frames with different video-level classes into the negative samples of the current frame.

For Video \mathbf{V}_b that has the same video-level class labels as Video \mathbf{V}_a ($y_a = y_b$), we define the paired contrastive loss for the i -th frame of Video V_a in the first view as follows:

$$L_{PCL,i}^1(V_a) = - \sum_{b \in S(a)} \sum_{j \in \mathbf{P}_i} \log \frac{\exp(\text{sim}(\mathbf{z}_{a,i}^1, \mathbf{z}_{b,j})/\tau)}{A_{i,j}} \quad (4)$$

$$A_{i,j} = \exp(\text{sim}(\mathbf{z}_{a,i}^1, \mathbf{z}_{b,j})/\tau) + \sum_{\hat{\mathbf{z}} \in \mathbf{N}_i} \exp(\text{sim}(\mathbf{z}_{a,i}^1, \hat{\mathbf{z}})/\tau)$$

1. We denote a and b as the indexes of videos in a batch, i and j as the indexes of frames in a video.

$S(a)$ is a set of videos that have the same video-level label with \mathbf{V}_a : $S(a) = \{b | y_a = y_b\}$. \mathbf{P}_i is the set of positive frames in V_b , and \mathbf{N}_i is the set of negative frames. $A_{i,j}$ is the denominator that contains the current positive sample $\mathbf{z}_{b,j}$ and negative samples for $\mathbf{z}_{a,i}^1$.

We treat the positive set \mathbf{P}_i as finding the corresponding frame for \mathbf{V}_a^1 . We use an alignment method that has been widely used in the time series literature, namely Dynamic Time Warping (DTW) [60]. DTW is a global alignment metric, taking into account entire sequences while aligning. However, a single DTW between two views is inaccurate. Therefore, we ensemble the information of all views in the two videos to increase the accuracy of the video alignment. Specifically, we calculate the cost matrix ($\text{cost}(\mathbf{u}, \mathbf{v}) = 1 - \text{sim}(\mathbf{u}, \mathbf{v})$) between each view of two videos: V_a^1 (V_a^2) of Video a and V_b^1 (V_b^2) of Video b . Then, we can get four cost matrices between these two videos. For each cost matrix ($T \times T$), we restore it to the cost matrix between the original videos ($|V1| \times |V2|$) using the sampling frame index sequence S and 2D linear interpolation. We regard the average of the four cost matrices as the final cost matrix c . In the above way, we can better describe the distance between each frame of the original two videos.

Then we use the dynamic time warping (DTW) method on the final cost matrix c and get the DTW matrix \mathbf{D} , which particularly solves the below cumulative distance function, as Equation 5 shown.

$$\mathbf{D}(i, j) = c(i, j) + \min\{\mathbf{D}(i-1, j), \mathbf{D}(i, j-1), \mathbf{D}(i-1, j-1)\}, \quad (5)$$

$\mathbf{D}(i, j)$ indicates the shortest cumulative distance at i -th frame of \mathbf{V}_a and j -th frame of \mathbf{V}_b .

After filling the DTW matrix, the optimal path can be found from $\mathbf{D}(|V_a|, |V_b|)$ to $\mathbf{D}(1, 1)$. Specifically, for each cell, we choose the smallest value among the three adjacent cells in greedy search: left, down, and diagonally to the bottom-left ones. The search stops when $\mathbf{D}(1, 1)$ is reached. At the same time, we use threshold filtering on the final cost matrix c to eliminate the corresponding frames with low similarity. We take the frames on the optimal path whose cost is less than the threshold ϵ_1 as the corresponding frames. These corresponding frames of the i -th frame are used as positive samples \mathbf{P}_i . Concretely, positive samples of two selected videos ($y_a = y_b$) are the frames that satisfy $c(i, j) \leq \epsilon_1$ and (i, j) in the optimal path of DTW matrix. ϵ_1 is the average value of the minimum top 5% in matrix c . Since the value of the distance matrix is not accurate at the beginning of network training, we use a warmup strategy to make the discrimination between positive and negative samples more stable and robust. That is, we initial the weights after doing self-supervised learning for 50 epochs and then use weakly-supervised learning to continue training. Meanwhile, we define protect frames to avoid instability, that is $c(i, j) \leq \epsilon_2$. ϵ_2 is the average value of the minimum top 10% in matrix c . We regard the remaining frames in V_b as negative samples \mathbf{N} .

In the same way, $L_{SCL,i}(V_a) = L_{SCL,i}^1(V_a) + L_{SCL,i}^2(V_a)$ and $L_{PCL,i}(V_a) = L_{PCL,i}^1(V_a) + L_{PCL,i}^2(V_a)$. Then the total

loss for Video V_a is as follows:

$$L(V_a) = \frac{1}{T} \sum_{i=1}^T [L_{SCL,i}(V_a) + \lambda L_{PCL,i}(V_a)] \quad (6)$$

where λ is a trade-off parameter. In addition, we add a video-level cross-entropy loss to the final loss, where the video token is used to predict the video label.

4 EXPERIMENTS

4.1 Datasets and Annotations

To validate the usefulness of our representation learning technique, we use three video datasets: PennAction [31], FineGym [21], and Pouring [15]. These datasets contain a diverse set of videos. While Pouring focuses more on human hands interacting with objects, PennAction and FineGym focus on humans doing sports or exercise. We compare our method with state-of-the-art on all three datasets. We do not use any annotation in the training phase, except for weakly supervised learning, and we only use video-level labels. Unless otherwise specified, all ablation studies are conducted on PennAction dataset.

4.1.1 PennAction Dataset

PennAction contains videos of humans doing various different sports or exercises. Following TCC [19], we use 13 categories of PennAction, which do not contain repetitive actions. In total, there are 1140 videos for training and 966 videos for testing. Each action set has 40 – 134 videos for training and 42 – 116 videos for testing. We obtain frame-level and video-level labels from LAV [18]. The video frames are from 18 to 663.

4.1.2 FineGym Dataset

FineGym is a recent large-scale fine-grained action recognition dataset. It was specifically designed to evaluate the ability of a representation learning method to parse and recognize the different phases of an action. We chunk the original YouTube videos according to the action boundaries so that each trimmed video data only describes a single action type (including Floor Exercise, Balance Beam, Uneven Bars, or Vault-Women). Finally, we obtained 3182 videos for training and 1442 videos for testing. And the number of video frames varies from 140 to 5153. FineGym provides two data splits according to the number of categories, namely FineGym99 with 99 sub-action classes and FineGym288 with 288 sub-action classes.

4.1.3 Pouring Dataset

In Pouring dataset, videos record the process of hand pouring water from one object to another. The phase labels (5 phase classes) are obtained from TCC [19]. Following TCC, we use 70 videos for training and 14 videos for testing. The video frames are from 186 to 797.

4.2 Evaluation Metrics

For unsupervised learning, we first optimize our network on the training set without using any labels. We Follow [15], [18], [19] to use three metrics on Pouring dataset: Phase Classification [19], Phase Progression [19] and Kendall’s Tau [19], while adding the Average Precision@K [18] on PennAction dataset to evaluate within each action category and average them across the 13 action categories. Following [17], we use fine-grained Action Classification to evaluate our method on the FineGym dataset. One drawback of Phase Progression and Kendall’s Tau are that they assume there are no repetitive frames/labels in a video. For the datasets we consider, this drawback is not a problem. As for weakly supervised learning, we use video-level labels in the training phase. Besides the above four metrics, we evaluate the representations using two other metrics: One-shot Phase Classification and Temporal Clustering.

4.2.1 Phase Classification

Phase Classification (or fine-grained Action Classification) is the averaged per-frame classification accuracy, implemented by training an SVM classifier on top of the frozen network features to predict the phase labels frame-level labels (phase class or sub-action category).

4.2.2 Phase Progression

Phase Progression measures the representation ability of progress. We fix the network, which is learned by our representation method, and then train a linear regressor to predict the phase progression values (timestamp distance between a query frame and phase boundaries) for all frames. Then it is computed as the average R-squared measure. The maximum value of this measure is 1.

4.2.3 Kendall’s Tau

Kendall’s Tau is a statistical measure that can determine how well-aligned two sequences are in time. It is calculated over every pair of frames in a pair of videos by sampling two frames in the first video and retrieving the corresponding nearest frames in the second video. At last, we check whether their orders are shuffled. A value of 1 implies the videos are perfectly aligned, while a value of -1 implies the videos are aligned in the reverse order. It does not need any extra training or finetuning.

4.2.4 Average Precision@K

Average Precision@K is computed as how many frames in the retrieved K frames have the same phase labels as the query frame. It measures the fine-grained frame retrieval accuracy. We report the results when $K = 5, 10, 15$. No more training or finetuning is needed.

4.2.5 One-shot Phase Classification

We take one video with phase labels and then classify the phase of other videos with the same action. Specifically, for each frame in the other videos, we find its nearest neighbor in the labeled video using our frame-wise representations. Then One-shot Phase classification is the ratio of the number of frames predicted to be the correct phase category and the number of total frames in the video with the same action. If the value is close to 1, the network can be used in phase annotation applications to some extent.

TABLE 1

Comparison with state-of-the-art methods on PennAction, using various evaluation metrics: *Phase Classification* (Classification), *Phase Progression* (Progress) and *Kendall's Tau* (τ). The top row results are from per-action models, i.e., separate models are trained for different actions. The results in the middle and bottom rows are obtained from training a single model for all actions.

Method	Training Strategy	Annotation	Classification	Progress	τ
TCC [19]	Per-action	Weakly	81.35	0.664	0.701
LAV [18]			84.25	0.661	0.805
SaL [49]	Joint	None	68.15	0.390	0.474
TCN [15]			68.09	0.383	0.542
Ours-SS			93.07	0.918	0.985
TCC [19]	Joint	Weakly	74.39	0.591	0.641
LAV [18]			78.68	0.625	0.684
GTA [17]			-	0.789	0.748
Ours-WS			93.53	0.922	0.989

4.2.6 Temporal Clustering

We perform K-means clustering on all frame features in each video and then compare the clustering results with the ground truth labels. We denote that a is the number of pairs with the same ground truth labels in the same clustering, and b is the number of pairs with different ground truth labels in different clustering. We utilize the Rand index score as the metric for clustering, as follows:

$$\text{RI} = \frac{a + b}{C_2^n} \quad (7)$$

where n is the number of frames, then C_2^n is the total number of pairs. It does not matter if the calculation is performed on ordered or unordered pairs as long as it is performed consistently.

4.3 Implementation Details

In self-supervised learning, we initialize ResNet-50 [38] with pre-trained by BYOL [28] and adopt it as the frame-wise spatial encoder. Unless otherwise specified, we use a 3-layer Transformer encoder [29] with 256 hidden size and 8 heads to model temporal context. We train the model using Adam optimizer [61] with learning rate 10^{-4} and weight decay 10^{-5} . We decay the learning rate with a cosine decay schedule without restarts [62]. We set $\sigma^2 = 10$ in the Gaussian distribution of timestamp distance and $\tau = 0.1$ in our loss as default. Following SimCLR [26], random image cropping, horizontal flip-ping, random color distortions, and random Gaussian blur are employed as the spatial augmentations. For our temporal data augmentations described in Section 3.2, we set hyper-parameters $\alpha = 1.5$ and $\beta = 20\%$. The video batch size is set as 4 (8 views), and our model is trained on 4 Nvidia V100 GPUs for 300 epochs. During training, we sample $T = 240$ frames for Pouring and FineGym, $T = 80$ frames for PennAction because of shorter videos. During testing, we feed the whole video into the model at once, without any temporal down-sampling. We L2-normalize the frame-wise representations for evaluation.

For weak supervision, we are consistent with self-supervised learning, except for the following aspects. Unlike self-supervised learning, we only use video-level labels. To reduce model instability at the beginning of training, we initialize the weights trained by self-supervised learning.

TABLE 2

Fine-grained frame retrieval results on PennAction.

Method	AP@5	AP@10	AP@15
TCN [15]	77.84	77.51	77.28
TCC [19]	76.74	76.27	75.88
LAV [18]	79.13	78.98	78.90
Ours-SS	92.23	92.10	91.82
Ours-WS	92.28	92.15	91.93

TABLE 3

One-shot Classification and Clustering evaluation on PennAction.

Method	One-shot Acc	Rand Index Score
TCN [15]	74.78	0.682
TCC [19]	73.64	0.683
LAV [18]	71.90	0.692
Ours-SS	88.23	0.736
Ours-WS	88.93	0.732

4.4 Quantitative Evaluation

4.4.1 Results on PennAction Dataset

On the PennAction dataset, our method is compared with state-of-the-art methods, as shown in Table 1 and Table 2. TCC [19] and LAV [18] train a separate model for each action results in 13 expert models for 13 action categories correspondingly ("Per-action" in Table 1). In contrast, our method only trains a unified expert model for all 13 action classes ("Joint" in Table 2). We used the average results of 13 models for the "per-action" training strategy in comparison.

Obviously, in Table 1, under different evaluation metrics, our methods do not only outperform the methods using the joint training strategy, but also outperform the methods adopting the per-action training strategy by a large margin. Even without the help of weak labels, our method is optimal. After using weak labels, our method further improved the three metrics of "*Phase Classification*", "*Phase Progression*", and "*Kendall's Tau*" by 0.46%, 0.004, and 0.004, respectively.

In Table 2, we report the results under the Average Precision@K metric, which measures the performance of fine-grained frame retrieval. We report the results of TCC [19] and LAV [18] under the per-action training strategy. It is also true in the following text unless otherwise specified. Surprisingly, although our model does not use paired data

TABLE 4

Comparison with the speed (samples per second) and memory cost (GBs) of different methods to train 80 frames on PennAction.

Method	Model	Speed	Memory	Classification
TCC [19]	ResNet+C3D	0.85	17.7	74.4
TCC [19]	FVE	3.23	2.4	86.3
LAV [18]	FVE	0.01	3.9	83.5
GTA [17]	FVE	0.01	3.9	86.7
Ours-SS	FVE	1.35	3.5	93.1
Ours-WS	FVE	1.22	3.5	93.5

TABLE 5

Comparison with state-of-the-art methods on FineGym, under the evaluation of *Fine-grained Action Classification*.

Method	FineGym99	FineGym288
D ³ TW [24]	15.28	14.07
SpeedNet [43]	16.86	15.57
TCN [15]	20.02	17.11
SaL [49]	21.45	19.58
TCC [19]	25.18	20.82
GTA [17]	27.81	24.16
Ours-SS	41.75	35.23
Ours-WS	43.62	36.86

in training, it can successfully find frames with similar semantics from other videos. For all methods in AP@K, Our method in the self-supervised version is at least +11% better than the previous methods. Furthermore, the weakly-supervised version can exceed the self-supervised version by +0.05%.

In order to verify that our method has more stability in learning better feature representation, we conducted the one-shot classification and clustering evaluation. The results are shown in Table 3. Our method surpassed the previous method by 9% in one-shot classification evaluation. When a video with a subaction label is given, our method can find videos of the same category more accurately, which is beneficial to automatic video annotation. Without subaction labels, we use the clustering evaluation to observe whether videos with the same category can be clustered into the same clustering and whether videos of different categories are not in the same clustering. We reported the Rand index score in Table 3. Our results are superior to previous methods by about 0.04.

In addition, we also compared the speed (samples per second) and memory cost (GB) of training 80 frames with different methods on the PennAction dataset. The results are evaluated on one V100 with batch size 2. To illustrate the effect of FVE on speed improvement, we replace the video encoder of the previous method with our FVE for comparison. As shown in Table 4, our FVE has faster speed, more negligible memory consumption, and more appealing performance. Compared to LAV and GTA with soft DTW, our method is more efficient and effective since we don't need to backpropagate gradients through DTW.

4.4.2 Results on FineGym Dataset

Table 5 summarizes the experimental results of Fine-grained Action Classification on FineGym99 and Fine-

TABLE 6

Comparison with state-of-the-art methods on Pouring.

Method	Classification	Progress	τ
TCN [15]	89.53	0.804	0.852
TCC [19]	91.53	0.837	0.864
LAV [18]	92.84	0.805	0.856
Ours-SS	93.73	0.935	0.992
Ours-WS	94.07	0.920	0.973

TABLE 7

Ablation study on different network architectures in self-supervised learning.

Encoder	Contrastive	Classification	Progress	τ
ResNet50	SCL	68.63	0.296	0.440
ResNet50+C3D	SCL	83.96	0.705	0.778
FVE	SimCLR	88.05	0.898	0.891
FVE	SCL	93.07	0.918	0.985

Gym288 datasets. Our method is superior to the other self-supervised [15], [43], [49] and weakly-supervised [17], [19], [24] methods. The performance of our method in the self-supervised manner exceeds the previous state-of-the-art method GTA [17] by +13.94% on FineGym99 and +11.07% on FineGym288. Using weak labels, we can further improve +13.94% on FineGym99 and +11.07% on FineGym288. The considerable performance improvement proves the effectiveness of our framework. The weakly-supervised methods, i.e., TCC [19], D3TW [24], and GTA [17], assume there exists an optimal alignment between two videos in the training set. However, for FineGym dataset, the set and order of sub-actions may differ even in two videos describing the same action. Therefore, the alignment predicted by these methods can be incorrect, which impedes learning.

4.4.3 Results on Pouring Dataset

As shown in Table 6, our method also achieves the best performance on a relatively small dataset, Pouring. These results further demonstrate the excellent generalization ability of our approach.

4.5 Ablation Study

In this section, we perform multiple experiments to analyze the different components of our framework. Unless otherwise specified, experiments are conducted on the PennAction dataset in the self-supervised manner.

4.5.1 Network Architecture

In Table 7, we explored the impact of encoder network architecture. "ResNet-50+Transformer" denotes our default frame-level video encoder introduced in Section 3.3. "ResNet-50 only" means that we remove the Transformer encoder in our network, and only use 2D ResNet-50 and linear transformation layers to extract the representation per frame. "ResNet-50+C3D" represents that two 3D convolutional layers [6] are added at the top of ResNet-50 before spatial pooling, which is the same as the model used in TCC [19] and LAV [18]. These models are all trained using

TABLE 8

Study on the effects of using different numbers of layers in Transformer encoder.

#Layers	Classification	Progress	τ
1	92.15	0.909	0.985
2	92.61	0.913	0.990
3	93.07	0.918	0.985
4	92.81	0.910	0.990

TABLE 9

Ablation study on learnable blocks of ResNet-50.

Learnable Blocks	Classification	Progress	τ
None	90.63	0.907	0.994
Block5	93.07	0.918	0.985
Block4+Block5	92.98	0.919	0.989

the proposed sequence comparison loss in Section 3.4. Our default network is superior to the other two networks due to the long-range dependency modeling ability of Transformers.

4.5.2 Layer Number of Transformer Encoder

Table 8 shows the study using different layers in the transformer. We find that as the number of layers increases, the classification of stages increases. However, the phase progression decreases slightly when there are too many layers. We use three layers by default.

4.5.3 Training Different Blocks of ResNet

In our implementation, ResNet-50 is pre-trained on ImageNet. In Table 9, we study the effects of finetuning different blocks of ResNet-50. The standard ResNet contains 5 blocks, namely *Block1-Block5*. "None" denotes that all layers of ResNet are frozen. "Block5" denotes we freeze the first four residual blocks of ResNet, and only make the last residual block learnable, which is our default setting. Similarly, "Block 4+Block 5" means we freeze the first three blocks and only train the last two blocks. Table 9 shows that encoding dataset-related spatial information is important ("None" vs. "Block 5"), and training more blocks does not lead to improvement ("Block5" vs. "Block4+Block5").

4.5.4 Applying Our Network to Other Methods

We study whether our frame-level video encoder (FVE) introduced in Section 3.3 can improve the performance of TCC [19] and TCN [15]. Specially, we replace the C3D-based network with our networks. Table 10 shows the results. We

TABLE 10

Applying our network to TCN and TCC. [†] denotes we re-implement the method and replace the network with ours. "Contrastive baseline" uses the corresponding frame at the other view as the positive sample.

Method	Classification	Progress	τ
TCN [†]	86.31	0.898	0.832
TCC [†]	86.35	0.899	0.980
Ours	93.07	0.918	0.985

TABLE 11

Ablation study on Gaussian variance σ^2 and the temperature τ in sequence contrastive loss.

Hyper-parameters	Classification	Progress	τ
$\tau=0.1, \sigma^2=1$	92.95	0.903	0.963
$\tau=0.1, \sigma^2=25$	92.03	0.922	0.993
$\tau=1.0, \sigma^2=10$	91.57	0.889	0.993
$\tau=0.3, \sigma^2=10$	92.13	0.903	0.992
$\tau=0.1, \sigma^2=10$	93.07	0.918	0.985

TABLE 12

Ablation study on whether ensemble the cost of views, the cost threshold ϵ_1 , and the trade-off λ in paired contrastive loss.

Hyper-parameters	Classification	Progress	τ
$\epsilon_1=5\%, \lambda=0.3$, w.o. view ensemble	93.05	0.906	0.991
$\epsilon_1=100\%, \lambda=0.3$	92.85	0.818	0.992
$\epsilon_1=20\%, \lambda=0.3$	93.03	0.910	0.991
$\epsilon_1=5\%, \lambda=1.0$	93.37	0.908	0.991
$\epsilon_1=5\%, \lambda=0.0$	93.10	0.891	0.990
$\epsilon_1=5\%, \lambda=0.3$	93.53	0.922	0.989

find that our proposed FVE can significantly improve the performance of their methods (compared with the results in Table 5). In addition, our method still maintains a significant performance gain, which attributes to the proposed sequence contrast loss.

4.5.5 Hyper-parameters of Sequence Contrastive Loss

We study the hyper-parameters in our sequence contrastive loss (see Equation 1), i.e., temperature parameter τ and Gaussian variance σ^2 . The variance σ^2 of the prior Gaussian distribution controls how the adjacent frames are semantically similar to the reference frames. As shown in Table 11, when the variance is too tiny ($\sigma^2 = 1$) or too large variance ($\sigma^2 = 25$), it will degrade performance. We use proper $\sigma^2 = 10$ by default. In addition, we observe an appropriate temperature ($\tau = 0.1$) facilitates the learning from hard negatives, which is consistent with the conclusion in SimCLR [26].

4.5.6 Hyper-parameters of Paired Contrastive Loss

We study the hyper-parameters in our paired contrastive loss (see Equation 3), i.e., the cost threshold ϵ_1 and the weight of paired contrastive loss λ . The cost threshold ϵ_1 controls the filtering of frames with too small a cost. And λ is a trade-off parameter between sequence contrastive loss and paired contrastive loss. As shown in Table 12, the performance is improved with ϵ_1 . Because we should not drop out valuable frames, the ϵ_1 should be tiny, and then the performance will be better. We evaluated λ from 0 to 1. When $\lambda = 0.3$, the performance is the best. We use proper $\epsilon_1 = 5\%$ and $\lambda = 0.3$ by default.

4.5.7 Study on Different Temporal Data Augmentations

We study the different temporal data augmentations described in Section 3.2, including maximum crop size α , overlap ratio β between two video views, and different sampling

TABLE 13

Ablation study on hyper-parameters of temporal data augmentations. Effects of maximum crop size α , overlap ratio β , and random sampling strategy are studied. The experiments are conducted on FineGym99 dataset.

α	Sampling	β (%)	FineGym99
0	Random	20	36.72
1.5			41.75
1			39.03
1.5	Even	20	38.44
1.5	Random	0	38.15
		20	41.75
		50	39.14
		80	37.94
		100	35.53

TABLE 14

Ablation studies on the number of training frames under different data protocols. The study is conducted on FineGym99 *Fine-grained Action Classification* task. ‘Supervised’ means all layers are trained with supervised learning.

% of Labeled Data \rightarrow	10	50	100
<i>Number of training frames:</i>			
80	27.10	32.78	34.02
160	30.28	36.46	38.06
240	33.53	39.89	41.75
480	31.46	37.92	39.45
Supervised	24.51	48.75	60.37

strategies, namely random sampling and even sampling. Table 13 shows the results. $\alpha = 0$ means we do not use the temporal data augmentations. From the table, we can see that the performance drops dramatically when we crop the video with a fixed length ($\alpha = 1$). The performance also decreases when we perform even sampling on the cropped clips. As described in Section 3.4, our sequence contrastive loss does not rely on frame-to-frame correspondence between two augmented views. Experimentally, constructing two views with $\beta = 100\%$ percent of overlapped frames degrades the performance, since the variety of augmented data decreases. In addition, we also observe the performance drops when two views are constructed independently ($\beta = 0\%$). The reason is that in this setting, the training may bring the representations of temporally distant frames closer, which hinders the optimization.

4.5.8 Number of Training Frames and Linear Evaluation Under Different Data Protocols

As described in Section 3.3, our network takes augmented views with T frames as input. We study the effects of different frame numbers T on FineGym99. Table 14 shows the results. We observe that taking long sequences as input is essential for frame-wise representation learning. However, a too large frame number degrades the performance. We thus set $T = 240$ by default. We also conduct linear evaluation under different data protocols. Concretely, we use 10%, 50%, and 100% labeled data to train the linear classifier. Compared with the supervised model (all layers are learnable), our method achieves better performance when the labeled data is limited (10% data protocol).

TABLE 15

Our CARL pre-trained on Kinetics-400 shows outstanding transfer ability on PennAction. Fine-tuning the pre-trained model on PennAction further boosts the performance.

Training Dataset	Methods	Classification	Progress	τ
PennAction	Ours-SS	93.0	0.918	0.985
PennAction	Ours-WS	93.5	0.922	0.989
K400	Ours-SS	91.9	0.903	0.949
K400 \rightarrow PennAction	Ours-SS	93.9	0.908	0.977



Fig. 5. Visualization of fine-grained frame retrieval on FineGym dataset by using our method.

4.5.9 Kinetics-400 Pre-training

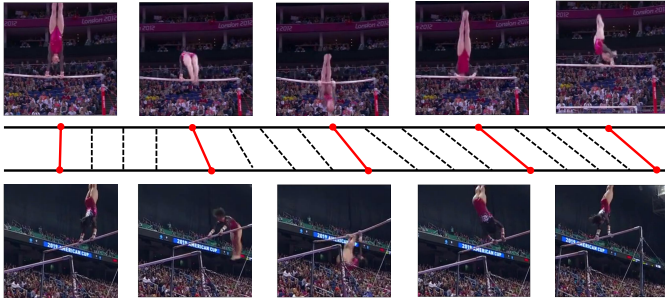
To show our method can benefit from large-scale datasets without any labels, we train our CARL on Kinetics-400 [2]. As Table 15 shows, the frame-wise representations trained on Kinetics-400 show outstanding generalization on PennAction dataset. Moreover, fine-tuning the pre-trained model on PennAction by using our CARL further boosts the performance, e.g., +2% classification improvement.

4.6 Quantitative Evaluation

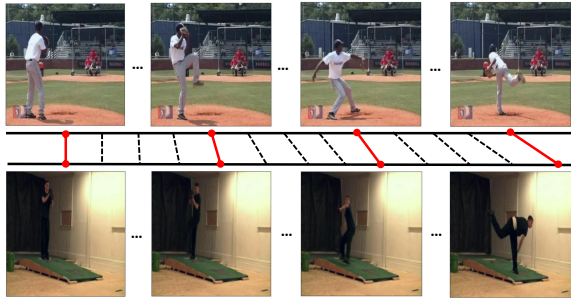
In this section, we present the visualization of multiple applications of our frame-wise representation learning, i.e., fine-grained frame retrieval, video alignment, and phase boundary detection. As shown in the figures, the representations obtained through our method (CARL) are invariant to the appearance, viewpoint, and background.

4.6.1 Fine-grained Frame Retrieval

Figure 5 shows the visualization results of fine-grained frame retrieval on FineGym and PennAction dataset. Specifically, we feed the video containing the query frame into our CARL framework to generate query features. Similarly, we can extract frame-wise features for the rest videos in the test set. We simply compute the cosine similarity between query features and frame-wise features from candidate videos to

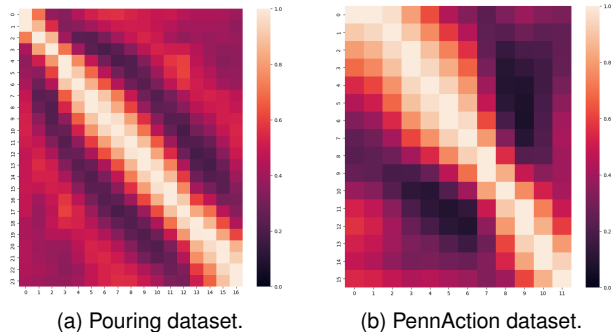


(a) Video Alignment of Artistic Gymnastics on FineGym dataset.



(b) Video Alignment of Baseball Game on PennAction dataset.

Fig. 6. Visualization of video alignment. Please refer to video demos in our supplementary materials for more visualization results.



(a) Pouring dataset.

(b) PennAction dataset.

Fig. 7. We randomly select two videos recording the same process (or action) from Pouring (or PennAction) dataset and compute the similarity matrix for frame-wise representations extracted by our method. The similarities are normalized for better visualization.

obtain top-5 retrieval frames, as shown in Figure 5. The retrieval frames have similar semantics with the query frame, although the appearance, camera view, and background are different, which suggests that our method is robust to these factors.

4.6.2 Video Alignment

Given two videos recording the same action or process, the goal of video alignment is to find the temporal correspondence between them. Figure 6 shows two examples from test set of FineGym and PennAction. Specially, we first use our framework to extract the frame-wise representations for two randomly selected videos. Then we compute the cosine similarities between the frame-wise representations of two videos and utilize the famous dynamic time warping (DTW) algorithm on the similarity matrix to find the best

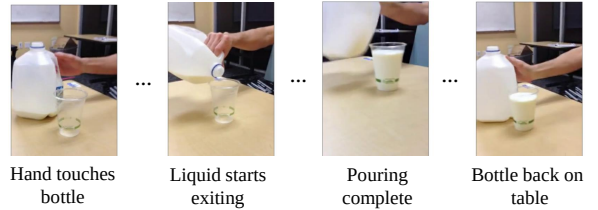


Fig. 8. Phase boundary detection on the Pouring dataset.

temporal alignment. Please refer to video demos in our supplementary materials for more visualization results.

We also randomly select two videos recording the same process (or action) from Pouring (or PennAction) dataset, and similarly, we can compute the similarity matrix which is rendered as a heatmap in Figure 7. We observe that the diagonal is highlighted, which means our approach find the favorable alignment between two correlated videos. We also give video demos in our supplementary materials.

4.6.3 Phase Boundary Detection

We can perform phase boundary detection by simply marking the boundaries of predicted phase classes. An example in the test set of the Pouring dataset is shown in Figure 8. Our method can accurately identify different phases in action, even if the similarity between these phases is high.

5 CONCLUSION

In this paper, we present a novel framework named contrastive action representation learning (CARL) to learn frame-wise action representations, especially for long videos, in a self-supervised or weakly-supervised manner. To considers both spatial and temporal context, we introduce a simple yet efficient network named frame-level video encoder (FVE) combining convolution and transformer. In addition, we propose a novel sequence contrastive loss (SCL) in two versions for frame-wise representation learning. One is the self-supervised version that optimizes the embedding space by minimizing the cross-entropy between the sequence similarity of two augmented views and a prior Gaussian distribution of timestamp distance. The other is the weakly-supervised version, SCL builds more sample pairs among videos using video-level labels by dynamic time warping (DTW). Experiments on various datasets and tasks show the effectiveness and generalization of our method.

REFERENCES

- [1] A. Arnab, M. Dehghani, G. Heigold, C. Sun, M. Lucic, and C. Schmid, "Vivit: A video vision transformer," *ArXiv*, 2021.
- [2] J. Carreira and A. Zisserman, "Quo vadis, action recognition? a new model and the kinetics dataset," in *CVPR*, 2017.
- [3] C. Feichtenhofer, H. Fan, J. Malik, and K. He, "Slowfast networks for video recognition," in *ICCV*, 2019.
- [4] D. Neimark, O. Bar, M. Zohar, and D. Asselmann, "Video transformer network," *ArXiv*, 2021.
- [5] K. Simonyan and A. Zisserman, "Two-stream convolutional networks for action recognition in videos," in *NIPS*, 2014.
- [6] D. Tran, L. D. Bourdev, R. Fergus, L. Torresani, and M. Paluri, "Learning spatiotemporal features with 3d convolutional networks," in *ICCV*, 2015.

- [7] X. Wang, R. B. Girshick, A. Gupta, and K. He, "Non-local neural networks," in *CVPR*, 2018.
- [8] Y. Xu, F. Wei, X. Sun, C. Yang, Y. Shen, B. Dai, B. Zhou, and S. Lin, "Cross-model pseudo-labeling for semi-supervised action recognition," *arXiv preprint arXiv:2112.09690*, 2021.
- [9] R. Goyal, S. E. Kahou, V. Michalski, J. Materzynska, S. Westphal, H. Kim, V. Haenel, I. Fründ, P. N. Yianilos, M. Mueller-Freitag, F. Hoppe, C. Thureau, I. Bax, and R. Memisevic, "The "something something" video database for learning and evaluating visual common sense," in *ICCV*, 2017.
- [10] K. Soomro, A. R. Zamir, and M. Shah, "Ucf101: A dataset of 101 human actions classes from videos in the wild," *ArXiv*, 2012.
- [11] N. C. Camgoz, S. Hadfield, O. Koller, H. Ney, and R. Bowden, "Neural sign language translation," in *CVPR*, 2018.
- [12] N. C. Camgoz, O. Koller, S. Hadfield, and R. Bowden, "Sign language transformers: Joint end-to-end sign language recognition and translation," in *CVPR*, 2020.
- [13] Y. Chen, F. Wei, X. Sun, Z. Wu, and S. Lin, "A simple multi-modality transfer learning baseline for sign language translation," *arXiv preprint arXiv:2203.04287*, 2022.
- [14] Y. Liu, A. Gupta, P. Abbeel, and S. Levine, "Imitation from observation: Learning to imitate behaviors from raw video via context translation," *2018 IEEE International Conference on Robotics and Automation (ICRA)*, 2018.
- [15] P. Sermanet, C. Lynch, Y. Chebotar, J. Hsu, E. Jang, S. Schaal, and S. Levine, "Time-contrastive networks: Self-supervised learning from video," *2018 IEEE International Conference on Robotics and Automation (ICRA)*, 2018.
- [16] K. Cao, J. Ji, Z. Cao, C. Chang, and J. C. Niebles, "Few-shot video classification via temporal alignment," in *CVPR*, 2020.
- [17] I. Hadji, K. G. Derpanis, and A. D. Jepson, "Representation learning via global temporal alignment and cycle-consistency," in *CVPR*, 2021.
- [18] S. Haresh, S. Kumar, H. Coskun, S. N. Syed, A. Konin, M. Z. Zia, and Q.-H. Tran, "Learning by aligning videos in time," in *CVPR*, 2021.
- [19] D. Dwibedi, Y. Aytar, J. Tompson, P. Sermanet, and A. Zisserman, "Temporal cycle-consistency learning," in *CVPR*, 2019.
- [20] H. Kuehne, A. B. Arslan, and T. Serre, "The language of actions: Recovering the syntax and semantics of goal-directed human activities," in *CVPR*, 2014.
- [21] D. Shao, Y. Zhao, B. Dai, and D. Lin, "Finegym: A hierarchical video dataset for fine-grained action understanding," in *CVPR*, 2020.
- [22] T. Yao, Y. Zhang, Z. Qiu, Y. Pan, and T. Mei, "Seco: Exploring sequence supervision for unsupervised representation learning," in *AAAI*, 2021.
- [23] M. Rohrbach, A. Rohrbach, M. Regneri, S. Amin, M. Andriluka, M. Pinkal, and B. Schiele, "Recognizing fine-grained and composite activities using hand-centric features and script data," in *IJCV*, 2015.
- [24] C. Chang, D.-A. Huang, Y. Sui, L. Fei-Fei, and J. C. Niebles, "D3tw: Discriminative differentiable dynamic time warping for weakly supervised action alignment and segmentation," in *CVPR*, 2019.
- [25] M. Caron, I. Misra, J. Mairal, P. Goyal, P. Bojanowski, and A. Joulin, "Unsupervised learning of visual features by contrasting cluster assignments," *ArXiv*, 2020.
- [26] T. Chen, S. Kornblith, M. Norouzi, and G. E. Hinton, "A simple framework for contrastive learning of visual representations," in *ICML*, 2020.
- [27] X. Chen, H. Fan, R. B. Girshick, and K. He, "Improved baselines with momentum contrastive learning," *ArXiv*, 2020.
- [28] J.-B. Grill, F. Strub, F. Altché, C. Tallec, P. H. Richemond, E. Buchatskaya, C. Doersch, B. Á. Pires, Z. D. Guo, M. G. Azar, B. Piot, K. Kavukcuoglu, R. Munos, and M. Valko, "Bootstrap your own latent: A new approach to self-supervised learning," *ArXiv*, 2020.
- [29] A. Vaswani, N. M. Shazeer, N. Parmar, J. Uszkoreit, L. Jones, A. N. Gomez, L. Kaiser, and I. Polosukhin, "Attention is all you need," in *NIPS*, 2017.
- [30] Z. Wu, Y. Xiong, S. X. Yu, and D. Lin, "Unsupervised feature learning via non-parametric instance discrimination," in *CVPR*, 2018.
- [31] W. Zhang, M. Zhu, and K. G. Derpanis, "From actemes to action: A strongly-supervised representation for detailed action understanding," in *ICCV*, 2013.
- [32] M. Chen, F. Wei, C. Li, and D. Cai, "Frame-wise action representations for long videos via sequence contrastive learning," in *CVPR*, 2022.
- [33] F. C. Heilbron, V. Escorcia, B. Ghanem, and J. C. Niebles, "Activitynet: A large-scale video benchmark for human activity understanding," in *CVPR*, 2015.
- [34] M. Monfort, B. Zhou, S. A. Bargal, A. Andonian, T. Yan, K. Ramakrishnan, L. M. Brown, Q. Fan, D. Gutfreund, C. Vondrick, and A. Oliva, "Moments in time dataset: One million videos for event understanding," *PAMI*, 2020.
- [35] G. A. Sigurdsson, G. Varol, X. Wang, A. Farhadi, I. Laptev, and A. Gupta, "Hollywood in homes: Crowdsourcing data collection for activity understanding," in *ECCV*, 2016.
- [36] G. Bertasius, H. Wang, and L. Torresani, "Is space-time attention all you need for video understanding?" *ArXiv*, 2021.
- [37] L. Wang, Y. Xiong, Z. Wang, Y. Qiao, D. Lin, X. Tang, and L. V. Gool, "Temporal segment networks for action recognition in videos," *PAMI*, 2019.
- [38] K. He, X. Zhang, S. Ren, and J. Sun, "Deep residual learning for image recognition," in *CVPR*, 2016.
- [39] J. Deng, W. Dong, R. Socher, L. Li, K. Li, and F. Li, "Imagenet: A large-scale hierarchical image database," in *CVPR*, 2009.
- [40] A. Dosovitskiy, L. Beyer, A. Kolesnikov, D. Weissenborn, X. Zhai, T. Unterthiner, M. Dehghani, M. Minderer, G. Heigold, S. Gelly, J. Uszkoreit, and N. Houlsby, "An image is worth 16x16 words: Transformers for image recognition at scale," in *ICLR*, 2021.
- [41] N. Carion, F. Massa, G. Synnaeve, N. Usunier, A. Kirillov, and S. Zagoruyko, "End-to-end object detection with transformers," *ArXiv*, 2020.
- [42] S. Jenni, G. Meishvili, and P. Favaro, "Video representation learning by recognizing temporal transformations," in *Computer Vision - ECCV 2020 - 16th European Conference, Glasgow, UK, August 23-28, 2020, Proceedings, Part XXVIII*, ser. Lecture Notes in Computer Science, A. Vedaldi, H. Bischof, T. Brox, and J. Frahm, Eds., vol. 12373. Springer, 2020, pp. 425–442. [Online]. Available: https://doi.org/10.1007/978-3-030-58604-1_26
- [43] S. Benaim, A. Ephrat, O. Lang, I. Mosseri, W. T. Freeman, M. Rubinstein, M. Irani, and T. Dekel, "Speednet: Learning the speediness in videos," in *CVPR*, 2020.
- [44] J. Wang, J. Jiao, and Y. Liu, "Self-supervised video representation learning by pace prediction," in *Computer Vision - ECCV 2020 - 16th European Conference, Glasgow, UK, August 23-28, 2020, Proceedings, Part XVII*, ser. Lecture Notes in Computer Science, A. Vedaldi, H. Bischof, T. Brox, and J. Frahm, Eds., vol. 12362. Springer, 2020, pp. 504–521. [Online]. Available: https://doi.org/10.1007/978-3-030-58520-4_30
- [45] Y. Yao, C. Liu, D. Luo, Y. Zhou, and Q. Ye, "Video playback rate perception for self-supervised spatio-temporal representation learning," in *2020 IEEE/CVF Conference on Computer Vision and Pattern Recognition, CVPR 2020, Seattle, WA, USA, June 13-19, 2020*. Computer Vision Foundation / IEEE, 2020, pp. 6547–6556. [Online]. Available: https://openaccess.thecvf.com/content_CVPR2020/html/Yao_Video_Playback_Rate_Perception_for_Self-Supervised_Spatio-Temporal_Representation_Learning_CVPR2020_paper.html
- [46] T. Han, W. Xie, and A. Zisserman, "Video representation learning by dense predictive coding," in *ICCVW*, 2019.
- [47] T. Pan, Y. Song, T. Yang, W. Jiang, and W. Liu, "Videomoco: Contrastive video representation learning with temporally adversarial examples," in *IEEE Conference on Computer Vision and Pattern Recognition, CVPR 2021, virtual, June 19-25, 2021*. Computer Vision Foundation / IEEE, 2021, pp. 11205–11214. [Online]. Available: https://openaccess.thecvf.com/content/CVPR2021/html/Pan_VideoMoCo_Contrastive_Video_Representation_Learning_With_Temporally_Adversarial_Examples_CVPR2021_paper.html
- [48] N. Behrmann, M. Fayyaz, J. Gall, and M. Noroozi, "Long short view feature decomposition via contrastive video representation learning," in *2021 IEEE/CVF International Conference on Computer Vision, ICCV 2021, Montreal, QC, Canada, October 10-17, 2021*. IEEE, 2021, pp. 9224–9233. [Online]. Available: <https://doi.org/10.1109/ICCV48922.2021.00911>
- [49] I. Misra, C. L. Zitnick, and M. Hebert, "Shuffle and learn: Unsupervised learning using temporal order verification," in *ECCV*, 2016.
- [50] Q. Kong, W. Wei, Z. Deng, T. Yoshinaga, and T. Murakami, "Cycle-contrast for self-supervised video representation learning," in

- Advances in Neural Information Processing Systems 33: Annual Conference on Neural Information Processing Systems 2020, NeurIPS 2020, December 6-12, 2020, virtual*, H. Larochelle, M. Ranzato, R. Hadsell, M. Balcan, and H. Lin, Eds., 2020. [Online]. Available: <https://proceedings.neurips.cc/paper/2020/hash/5c9452254bccd24b8ad0bb1ab4408ad1-Abstract.html>
- [51] K. Sohn, "Improved deep metric learning with multi-class n-pair loss objective," in *Advances in Neural Information Processing Systems 29: Annual Conference on Neural Information Processing Systems 2016, December 5-10, 2016, Barcelona, Spain*, D. D. Lee, M. Sugiyama, U. von Luxburg, I. Guyon, and R. Garnett, Eds., 2016, pp. 1849–1857. [Online]. Available: <https://proceedings.neurips.cc/paper/2016/hash/6b180037abbebea991d8b1232f8a8ca9-Abstract.html>
 - [52] A. van den Oord, Y. Li, and O. Vinyals, "Representation learning with contrastive predictive coding," *CoRR*, vol. abs/1807.03748, 2018. [Online]. Available: <http://arxiv.org/abs/1807.03748>
 - [53] T. Han, W. Xie, and A. Zisserman, "Memory-augmented dense predictive coding for video representation learning," in *Computer Vision - ECCV 2020 - 16th European Conference, Glasgow, UK, August 23-28, 2020, Proceedings, Part III*, ser. Lecture Notes in Computer Science, A. Vedaldi, H. Bischof, T. Brox, and J. Frahm, Eds., vol. 12348. Springer, 2020, pp. 312–329. [Online]. Available: https://doi.org/10.1007/978-3-030-58580-8_19
 - [54] N. Behrmann, J. Gall, and M. Noroozi, "Unsupervised video representation learning by bidirectional feature prediction," in *IEEE Winter Conference on Applications of Computer Vision, WACV 2021, Waikoloa, HI, USA, January 3-8, 2021*. IEEE, 2021, pp. 1669–1678. [Online]. Available: <https://doi.org/10.1109/WACV48630.2021.00171>
 - [55] F. Wei, Y. Gao, Z. Wu, H. Hu, and S. Lin, "Aligning pretraining for detection via object-level contrastive learning," *Advances in Neural Information Processing Systems*, vol. 34, 2021.
 - [56] C. Feichtenhofer, H. Fan, B. Xiong, R. B. Girshick, and K. He, "A large-scale study on unsupervised spatiotemporal representation learning," in *CVPR*, 2021.
 - [57] H. Kuang, Y. Zhu, Z. Zhang, X. Li, J. Tighe, S. Schwertfeger, C. Stachniss, and M. Li, "Video contrastive learning with global context," *ArXiv*, 2021.
 - [58] R. Qian, T. Meng, B. Gong, M.-H. Yang, H. Wang, S. J. Belongie, and Y. Cui, "Spatiotemporal contrastive video representation learning," in *CVPR*, 2021.
 - [59] K. Li, X. Sun, Z. Wu, F. Wei, and S. Lin, "Towards tokenized human dynamics representation," *arXiv preprint arXiv:2111.11433*, 2021.
 - [60] D. J. Berndt and J. Clifford, "Using dynamic time warping to find patterns in time series," in *Knowledge Discovery in Databases: Papers from the 1994 AAAI Workshop, Seattle, Washington, USA, July 1994. Technical Report WS-94-03*, U. M. Fayyad and R. Uthurusamy, Eds. AAAI Press, 1994, pp. 359–370.
 - [61] D. P. Kingma and J. Ba, "Adam: A method for stochastic optimization," in *3rd International Conference on Learning Representations, ICLR 2015, San Diego, CA, USA, May 7-9, 2015, Conference Track Proceedings*, Y. Bengio and Y. LeCun, Eds., 2015. [Online]. Available: <http://arxiv.org/abs/1412.6980>
 - [62] I. Loshchilov and F. Hutter, "Sgdr: Stochastic gradient descent with warm restarts," *arXiv: Learning*, 2017.